CommIT Journal 20(1), 29–44, 2026

Magnetic Resonance Imaging (MRI)-Based Breast Cancer Detection Using Graph Convolutional Network (GCN) with Advanced Texture Feature Extraction

Ferdaus Anam Jibon[1], Sujan Chandra Roy[2], Hadia Razin Mou[3], Md. Ashraful Islam[4*], Utpal Kanti Das[5], Ripa Sarkar[6], and Ratna R. Sarkar[7]
[1,5]Department of Computer Science and Engineering,
IUBAT - International University of Business Agriculture and Technology
Dhaka, Bangladesh 1230
[2]Institute of Information and Communication Technology,
Chittagong University of Engineering and Technology
Chattogram, Bangladesh 4349
[3]Department of Computer Science and Engineering,
University of Information Technology and Sciences
Dhaka, Bangladesh 1212
[4]Department of Information and Communication Engineering, University of Rajshahi
Rajshahi, Bangladesh 6205
[6]Department of Computer Science and Engineering, Uttara University
Dhaka, Bangladesh 1230
[7]Department of Computer Science and Engineering, National University
Gazipur, Bangladesh 1704
Email: [1]jibon.cse@iubat.edu, [2]sujan.007.ice@gmail.com, [3]hrmou1111@gmail.com,
[4]ras_ice@ru.ac.bd, [5]ukd@iubat.edu, [6]ripa.sarkar@uttarauniversity.edu.bd, [7]ratna.rani@nu.ac.bd

***Abstract*—Breast cancer is the leading cause of death for women worldwide, and it is predicted to be an important factor in public health. Therefore, early and accurate detection is crucial to enhancing survival rates. Recently, Magnetic Resonance Imaging (MRI) has become a superior option to biopsies due to its exceptional soft tissue imaging capabilities, making it highly effective for detecting and monitoring breast cancer. However, it requires a competent radiologist to perform the procedure. The researchers introduce an approach for breast cancer detection and classification that employs Graph Convolutional Networks (GCNs) to distinguish breast MRI images. The combination of Dual-Tree Discrete Wavelet Transform (DTDWT) with GCNs enhances feature extraction, while the Gray-Level Co-Occurrence Matrix (GLCM) identifies texture patterns distinguishing normal, benign, and malignant tissues. The research also employs t-Distributed Stochastic Neighbor Embedding (t-SNE) for dimensionality reduction, improving pattern interpretation. This approach classifies the four breast cancer types using a dataset comprising 200 Dynamic Contrast-Enhanced (DCE)-MRI images from Radiopaedia, allocated as 160 training and 40 validation instances in categories including Ductal Carcinoma (DC), lipoma, Triple-Negative Breast Cancer (TNBC), and Inflammatory Breast Cancer (IBC). A comparative analysis confirms the validity of the approach, which is the first to address these four categories in MRI. The experimental results indicate significant improvements, achieving an accuracy of 0.9821 in classifying breast tumors as benign or malignant, thereby establishing a new diagnostic standard.**

***Index Terms*—Breast Cancer, Gray-Level Co-Occurrence Matrix (GLCM), Graph Convolutional Network (GCN), t-Distributed Stochastic Neighbor Embedding (t-SNE), Dual-Tree Discrete Wavelet Transform (DTDWT)**

Received: June 14, 2025; received in revised form: Aug. 27, 2025; accepted: Aug. 29, 2025; available online: March 05, 2026.
*Corresponding Author

I. Introduction

RECENTLY, breast cancer has become one of the most common cancers and is a leading cause of

death for women worldwide. According to the World Health Organization (WHO), there are a significant number of women diagnosed with breast cancer every year. In 2020, there were approximately 2.3 million women worldwide diagnosed with the disease, and 685,000 died as a result. Due to the rising trend of this number, it is crucial to have prompt and effective detection and treatment strategies [1, 2]. Breast cancer results from the abnormal and unchecked growth of cells within breast tissue, which can invade surrounding tissues and spread to other parts of the body. Benign tumors tend to develop locally and are not cancerous, while malignant tumors are cancerous and can grow out of control [3, 4]. Therefore, the early detection of breast cancer is a crucial factor that contributes significantly to the reduction in women's mortality rate due to this disease. Breast cancer screening has previously included mammography, histopathology, Magnetic Resonance Imaging (MRI), ultrasound, and thermography as imaging methods [5, 6].

However, interpreting medical images is a challenging task for multiple reasons, including overlapping breast tissues, variations in mass shapes and sizes, and the similarity in appearance between benign and malignant lesions [7]. False negative cases or overlooked cancers can delay diagnosis and treatment, whereas false positives or misidentifications can lead to unnecessary treatment [8]. With increasing success, radiologists are utilizing Machine Learning (ML) and Deep Learning (DL) techniques to successfully address these challenges and achieve faster and more precise breast cancer detection. These advanced approaches not only enhance diagnostic accuracy but also significantly improve patient outcomes, underscoring their critical role in the fight against breast cancer. Unlike radiologists, who analyze isolated regions, AI examines medical images globally at the pixel level, enhancing diagnostic accuracy [9].

ML-based breast cancer classification typically follows four steps: pre-processing, feature extraction, model training, and classification. Many variations of these three steps can be used to attain a good result. For instance, methods, such as Biogeography-Based Optimization (BBO), Decision Trees (DT), Fractional Fourier Transform (FrFT), K-Nearest Neighbor (kNN), Particle Swarm Optimization (PSO), Support Vector Machines (SVM), and Wavelet Energy Entropy (WEE), have been widely used in mammographic breast cancer detection [10–12]. Another previous research has performed an extensive examination of machine learning models designed to predict breast cancer risks, employing algorithms including SVM, Random Forest, KNN, and Logistic Regression. Their models are able to achieve 99.7% accuracy, precision, and recall, with SVM outperforming others in most metrics, to identify critical features and optimize prediction performance for early and reliable detection of breast cancer [13].

Previous research has introduced a new breast cancer diagnosis method called SNSVM, which combines SqueezeNet and SVM. The method gathers relevant information from mammography images using SqueezeNet and classifies them with SVM. The method achieves 94.10% accuracy and 94.30% sensitivity, having a superior performance over state-of-the-art models, while also boosting early detection of malignant cases with high computational efficiency [14]. Another study has proposed a hybrid technique for detecting breast cancer earlier by integrating ResNet152 for feature extraction and SVM for classification. The approach achieves an accuracy of 97.62%, a recall of 98.53%, and a specificity of 94.52%. The main objective of the proposal is to enhance early diagnosis by capturing subtle thermal variations that indicate malignant tissues [15].

DL techniques, particularly Convolutional Neural Networks (CNNs), have gained significant attention for breast cancer detection due to their ability to learn hierarchical features directly from images. Their performance is closely linked to the availability of large datasets, which enable them to outperform traditional ML algorithms on complex tasks [16–19]. Several studies have combined CNNs with optimization and ensemble techniques to enhance performance. ResNet-18, ShuffleNet, and Inception-V3Net have achieved binary classification accuracies exceeding 99% and multi-class accuracies above 95% on benchmark datasets such as BreakHis [20]. Another study has utilized a graph-based approach to represent ultrasound images as nodes in a graph, weighted by Spearman correlation coefficients, and applied a Graph Neural Network (GNN), achieving over 99% accuracy, precision, and recall [21].

In addition to CNNs, graph models like GCNs have become a powerful alternative for handling structured data and capturing relational dependencies. GCNs utilize both node features and graph topology, which enables better representation learning on medical datasets [22]. Previous research has proposed a hybrid approach integrating GCNs with CNNs, developing a novel framework called BDR-CNN-GCN. The proposed methodology utilizes Batch Normalization (BN) and Drop-Out (DO) to optimize the model, resulting in exceptional performance metrics that exceed 96% in accuracy, sensitivity, and specificity [23].

Although advances have been made, there are still challenges that need to be overcome to develop models

Cite this article as: F. A. Jibon, S. C. Roy, H. R. Mou, M. A. Islam, U. K. Das, R. Sarkar, and R. R. Sarkar, "Magnetic Resonance Imaging (MRI)-based breast cancer detection using Graph Convolutional Network (GCN) with advanced texture feature extraction", CommIT Journal 20(1), 29–44, 2026.

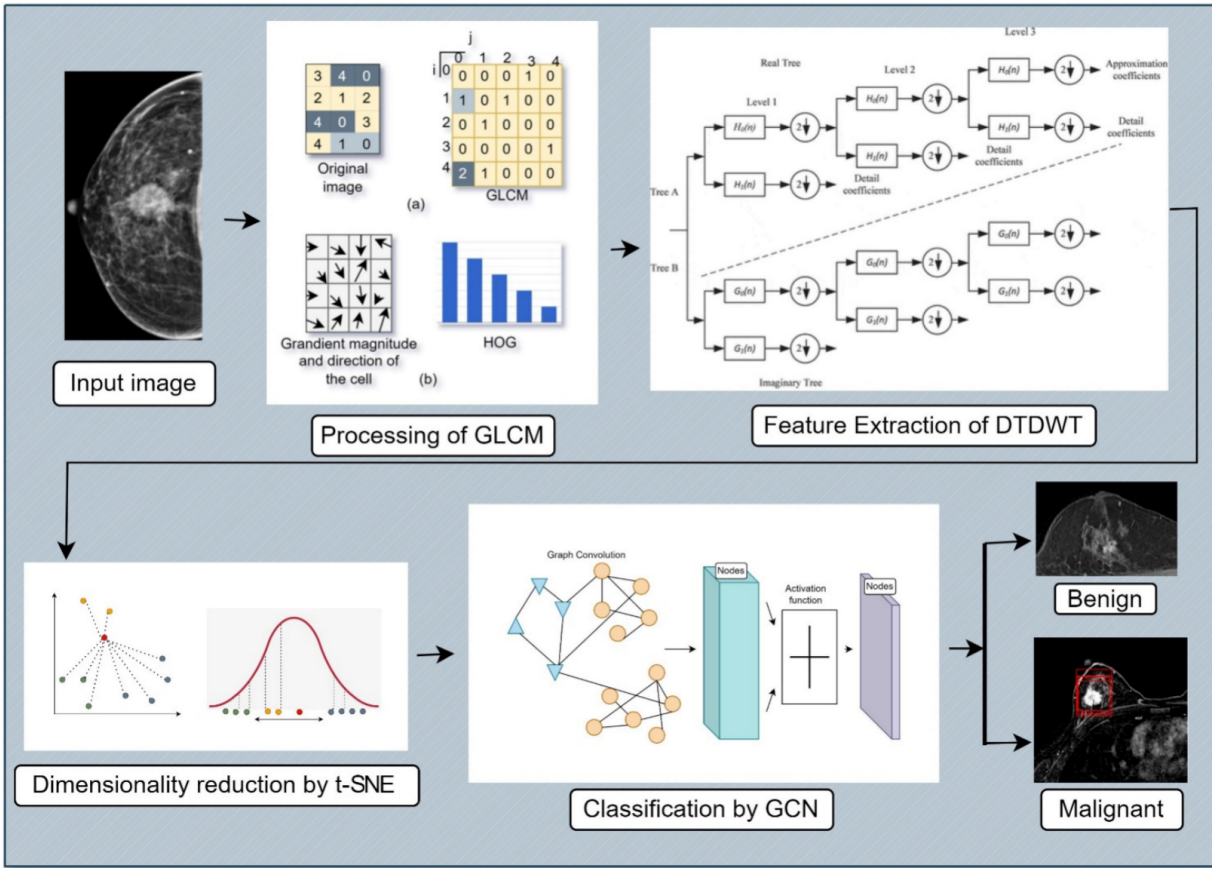

Fig. 1. Proposed model for breast cancer detection and classification. Note: Gray-Level Co-Occurrence Matrix (GLCM), Graph Convolutional Network (GCN), t-Distributed Stochastic Neighbor Embedding (t-SNE), Dual-Tree Discrete Wavelet Transform (DTDWT), and Histogram of Gradients (HOG)

that capture both fine-grained texture details and global structural information in medical images. Texture analysis methods like the Gray-Level Co-occurrence Matrix (GLCM) are widely used for extracting statistical features from image textures, but the Dual-Tree Discrete Wavelet Transform (DTDWT) can be utilized to enhance this process by conserving edges and details, which are crucial in determining whether a tissue is benign or malignant. The integration of advanced feature extraction techniques with DL architectures such as GCNs for breast cancer detection has not been examined in any prior studies, to researchers' knowledge.

To address the aforementioned issues, a novel graph-based hybrid framework is proposed for breast cancer detection from MRI images. The proposal employs GLCM's texture analysis and DTDWT's edge preservation with GCNs to secure effective feature representation and classification. In addition, t-Distributed Stochastic Neighbor Embedding (t-SNE) is utilized to increase feature visibility and reduce dimensionality. The proposed framework is designed to precisely detect and categorize four breast cancer types, such as Ductal Carcinoma (DC), lipoma, Triple-Negative Breast Cancer (TNBC), and Inflammatory Breast Cancer (IBC).

II. Research Method

A. Proposed Model

The ability to detect breast cancer in a timely and accurate manner is crucial for maximizing patient survival rates. Prioritizing early diagnosis ensures the best possible outcomes. This research presents a decisive four-phase process that starts with enhancing image coverage to improve data quality, as shown in Fig. 1. The MRI images are resampled (interpolating with 512×512 pixels), converted to grayscale, and normalized to remove color information while preserving luminance.

Since breast cancer has many variations, the research utilizes a method that is a combination of GLCM and DTDWT in feature extraction. DTDWT-based features

are frequency-based, and GLCM-based features are texture-based, thus giving an overall representation of the data. Then, subsequently, t-SNE is used to reduce the dimensionality of the extracted features. Finally, GCN has been applied to determine whether the cancer is benign or malignant.

Breast MRI images are often corrupted with noise, go through intensity inhomogeneities, and have structural diversity. This situation is where a combination of pre-processing and feature extraction, which converts high-dimensional features into low-dimensional features, comes into play. The GCN model achieves high classification accuracy due to its robustness in the training set created by extracting both texture and frequency features. It helps to improve diagnostic outcomes by combining solid cancer tissue classifiers into complementary multimodal features for robust prediction of cancer type.

B. Preprocessing

All images are resized to a uniform resolution of 256×256 pixels. To eliminate hue and saturation while preserving luminance, the images are converted from Red, Green, Blue (RGB) to grayscale. This preprocessing step ensures consistency and enhances the quality of the image data for subsequent analysis.

C. Segmentation

Segmentation is the process of separating objects from the background in an image. The research uses it to divide digital mammograms into non-overlapping regions to distinguish between benign and malignant masses from the background. The identification of breast masses is achieved by employing various algorithms, which include region-based methods, histogram-based methods, Markov Random Field (MRF), cluster-based methods, template matching methods, edge detection methods, and others. The K-means clustering technique, a commonly used segmentation technique, is applied to investigate and examine the detailed structures of the breast images in the experiment, which enables the pinpointing of regions of interest with precision.

D. Feature Extraction

The extraction of features is crucial in image processing and computer vision tasks, as it facilitates the efficient extraction of useful information from large amounts of image data for multiple applications. For effective classification, features need to be discriminating, computationally efficient, and mutually independent. Histogram of Gradients (HOG), GLCM, and Local Binary Pattern (LBP) are widely used feature extraction methods. LBP can capture texture by studying local pixel patterns, HOG provides information about object shapes through gradient orientation histograms, and GLCM identifies texture by analyzing spatial relationships between pixel intensities. Generally, in breast MRI images, features can be widely categorized into three types: (i) shape-based features (e.g., area, circularity, irregularity shape index, perimeter, and others), (ii) intensity-based features (e.g., mean, median, variance, skewness, range, standard deviation, kurtosis, pixel orientation, and others), and (iii) texture-based features (e.g., contrast, entropy, correlation, cluster shade, inertia, inverse difference moment, cluster prominence, energy, and others). Feature is extracted by the following methods. The first one is the intensity normalization that ensures consistent brightness and contrast across images. Intensity values are internally normalized using Eq. (1). Here I, μ and σ stand for pixel intensity, intensity, and standard deviation, respectively.

$$I_{norm} = \frac{I - \mu}{\sigma}. \tag{1}$$

The next one is the GLCM. It is a statistical tool widely used for extracting and analyzing textures from images. GLCM evaluates the spatial relationship between two pixel intensities and, based on that, provides a statistical measure of texture features. Analyzing the frequency of pixels at distance d and angle θ, GLCM can extract distinctive features that characterize the texture of the image [24].

Let $(x_1,\ y_1)$ and $(x_2,\ y_2)$ be two pixel positions separated by the distance d and angle θ. The intensity of a pixel at (x, y) is given by $I(x, y)$. Based on each pixel of an image, GLCM operates by forming a matrix where an element $(m,\ n)$ is the frequency of pixels with intensities m and n occurring at a specified relative spatial position. The mathematical representation of the matrix is given in Eq. (2).

$$P(i,j) = \frac{\|\{(x_1,y_1),(x_2,y_2) \mid I(x_1,y_1) = i, I(x_2,y_2) = j\}\|}{\text{Number of Pixel Pairs}} = \frac{\text{Number of Pixel Pairs}}{\text{Number of Pixel Pairs}}. \tag{2}$$

After the matrix is calculated, it is often normalized to ensure robustness against image size and intensity variation. A common normalization technique is to divide each member in the matrix by the total sum of elements. The normalized matrix is in Eq. (3).

$$NP(m,n) = \frac{P(m,n)}{\sum_m \sum_n P(m,n)}. \tag{3}$$

To capture the texture characteristics, several statis-

tical measures can be used in the GLCM. Commonly used features include:

- Energy: The uniformity of pixel intensity distribution can be achieved by having higher energy values, as shown in Eq. (4):

$$\text{Energy} = \sum_m \sum_n P(m,n)^2. \tag{4}$$

- Contrast: The high intensity difference between neighboring pixels implies substantial variation in Eq. (5):

$$\text{Contrast} = \sum_m \sum_n (m-n)^2 . P(m,n). \tag{5}$$

- Homogeneity: The proximity of elements in the GLCM to its diagonal represents similarity in pixel intensity in Eq. (6):

$$\text{Homogeneity} = \sum_m \sum_n \frac{P(m,n)}{1+|m-n|}. \tag{6}$$

- Entropy: The entropy is affected by the texture's randomness or complexity, as in Eq. (7):

$$\text{Entropy} = -\sum_m \sum_n P(m,n). \log P(m,n). \tag{7}$$

- Correlation: A linear relationship exists between pixel intensities, and high correlation values indicate strong dependency in Eq. (8). Here, μ_x, μ_y are the means, and σ_x, σ_y are the standard deviations of the GLCM row and column distribution.

$$\text{Cor} = \frac{\sum_m \sum_n mn.P(m,n)}{\sigma_x \sigma_y}. \tag{8}$$

The third one is DTDWT. It is a more advanced version of the classic Discrete Wavelet Transform (DWT) method. DTDWT has been designed to address limitations of DWT like aliasing and distortion, which allows it to more effectively extract characteristics of signals. To decompose a signal into its approximation and detail components, DTDWT constructs two parallel wavelet trees. Each of the components represents a specific frequency band. Let ψ and ϕ be the wavelet and scaling function. Then, the decomposition of a mammographic image $I(x,y)$ can be depicted in Eqs. (9) and (10).

$$A = \sum_{m,n} I(x,y). \phi(x-m)\phi(y-n), \tag{9}$$

$$D(m,n) = \sum_{m,n} I(x,y). \psi(x-m(x,y)\psi(y-n). \tag{10}$$

The A and D represent approximation coefficients and detail coefficients, while m and n represent image dimensions, as part of the decomposition process, traditional DWT uses 1/2 down sampling, which reduces the resolution of the signal without removing high-frequency components. These high-frequency components can fold into lower frequencies, creating unwanted artifacts and aliasing distortion. DTDWT overcomes this by performing complementary downsampling between the two parallel wavelet trees.

The fourth one is t-SNE. The t-SNE dimensionality reduction algorithm is employed to transfer high-dimensional data to a low-dimensional space while ensuring that Euclidean Distances (ED) are retained as much as possible. It makes it an ideal tool for clustering and visualization. First, the algorithm turns the ED into conditional probabilities (P_{ij}) between data points, which indicates the similarities between pairs, as indicated in Eq. (11). x_i and x_j are the data points in the high-dimensional space. The σ_i represents the bandwidth of the Gaussian distribution.

$$P_{mn} = \frac{\exp(-||x_i - x_j||^2/2\sigma_m^2)}{\sum_{k=l} \exp(-||x_k - x_l||^2/2\sigma_k^2)}. \tag{11}$$

Second, it is in the lower-dimensional space. The similarities are modelled by the t-distribution as indicated in Eq. (12). The y_i and y_j are the mapped points in the lower-dimensional space.

$$Q_{mn} = \frac{(1+||y_m - y_n||^2)^{-1}}{\sum_{k=l}(1+||y_k - y_l||^2)^{-1}}. \tag{12}$$

Third, the t-SNE algorithm works by minimizing the Kullback-Leibler (KL) divergence. Therefore, it brings the two distributions closer together, as indicated in Eq. (13). This optimization process ensures that the local structure of the data is preserved during the dimensionality reduction.

$$KL(P||Q) = \sum_m \sum_n P_{mn} \log\left(\frac{P_{mn}}{q_{mn}}\right). \tag{13}$$

The last one is GCN. GCN utilizes spectral graph theory and message-passing frameworks to expand the use of traditional CNNs beyond Euclidean spaces. The main concept of GCN is based on the graph representation of data, with nodes representing pixels or Region of Interests (ROIs) in an MRI image, and edges indicating spatial, textural, or functional relations between them. GCN is used to make more accurate decisions in breast cancer detection, as shown in Fig. 2.

In breast MRI, GCNs are adept at modelling hierarchical spatial relationships (e.g., tumor boundaries, parenchymal distortion) and multimodal correlations (e.g., T1/T2-weighted, Diffusion-Weighted Imaging (DWI), or Dynamic Contrast-Enhanced (DCE) sequences) with the help of adaptive graph structures. For instance, nodes can represent super pixels with features derived from intensity, texture, or pharmacokinetic

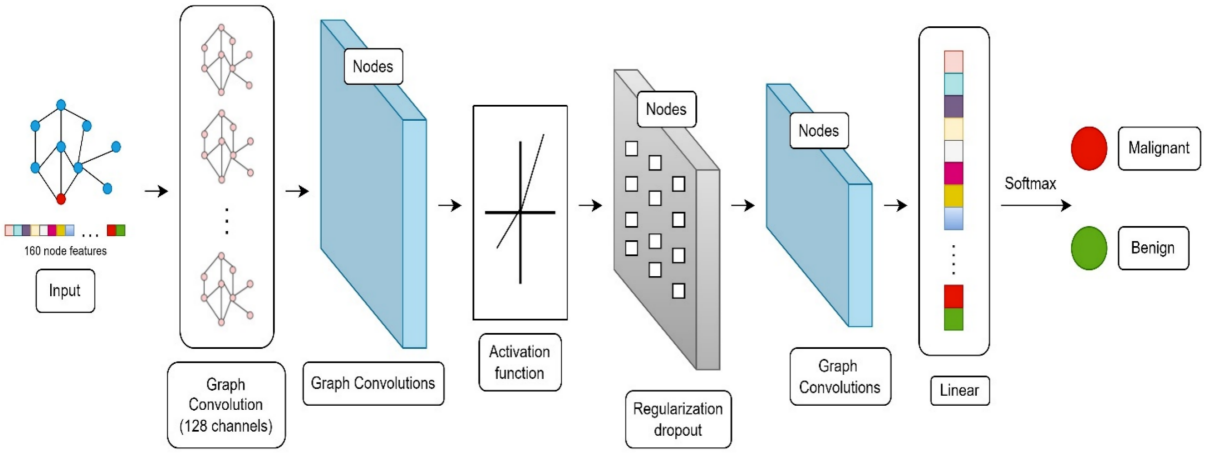

Fig. 2. Graph Convolutional Network (GCN) for breast cancer classification.

TABLE I
DESCRIPTION OF MAGNETIC RESONANCE IMAGING (MRI) IMAGES FOR DUCTAL CARCINOMA (DC), LIPOMA, TRIPLE-NEGATIVE BREAST CANCER (TNBC), AND INFLAMMATORY BREAST CANCER (IBC).

Classification	Training		Validation	
	Benign	Malignant	Benign	Malignant
Cancer Classification	100	60	24	16

parameters, while edges encode proximity or similarity in enhancement profiles.

E. Dataset Formation

The research relies on data from MRI datasets obtained from Radiopaedia (https://radiopaedia.org/articles/breast-mri). The datasets consist of well-organized mammograms labeled by a group of expert radiologists of DCE-MRI images. The cleaned dataset has 200 images with four categories of breast cancer: DC, lipoma, TNBC, and IBC, shown in Table I.

DC is a form of cancer that happens when abnormal cells develop in the lining of the milk duct and spread beyond the walls of the duct. The grade of DC can be determined by how closely the cancer cells resemble noncancerous cells, with grade 1 being well-differentiated, grade 2 being moderately differentiated, and grade 3 being poorly differentiated [25, 26].

The formation of lipoma is caused by an overgrowth of fat cells, which is non-cancerous and benign. The development of these growths is commonly observed in the fatty subcutaneous tissue. Soft and minimally painful lipomas normally exist as movable lumps that lack a defined form. Medical evaluation can confirm the benign nature, even though lipomas create no health danger [27].

TNBC is recognized as the most aggressive subtype of invasive breast cancer. Unlike other types, TNBC grows and metastasizes at a faster rate, making it more difficult to treat. Because of its rapid progression and limited treatment options, TNBC is classified as a very aggressive type of breast cancer and requires prompt and targeted intervention [28, 29].

IBC is a rare and highly aggressive type of breast cancer that results in the obstruction of lymphatic vessels in the breast skin by cancer cells. The term 'inflammatory' describes the typical symptoms of breast swelling, redness, and inflammation that give the breast its distinctive appearance. The majority of IBC cases are classified as invasive ductal carcinoma, as they originate from the cells that line the breast ducts and then spread to other areas [30].

F. Design Simulation

The implementation environment is built at Google Colab using Python 3.10, Pytorch version 2.0.1, PyTorch Geometric version 2.4.0, and CUDA. This setup provides enough computational resources to conduct the evaluation experiments efficiently.

For the experiments, input images in *png, *jpg, and *bmp formats are accepted. To ensure device compatibility, the input images are transformed into a suitable color space. Then, using K-means clustering in *a*b space, three color clusters are generated. The calculated pixel distances within these clusters are based on the ED metric. Following the clustering process, each pixel in the image receives labels from the K-means results, which result in an RGB-labeled image. This method results in a clear and efficient

workflow by systematically organizing and analyzing the clustered image data.

A combination of GLCM and DTDWT is utilized to extract features from a test image due to the diverse nature of breast cancer. The framework is developed to extract texture and multi-resolution features from breast cancer images, including mammograms, to identify benign tumors and those that are malignant. Thirteen features are retrieved from the given image: (1) contrast, (2) energy, (3) correlation, (4) mean, (5) homogeneity, (6) entropy, (7) standard deviation, (8) variance, (9) Root Mean Square (RMS), (10) skewness, (11) smoothness, (12) Inverse Differential Motion (IDM), and (13) kurtosis. The training dataset for DC, Lipoma, TNBC, and IBC images is organized into a 160×13 matrix. To accurately classify breast cancer, the validation set images have been arranged into a 40×13 matrix using a systematic approach. It ensures a comprehensive and structured dataset for each category.

The GLCM features are obtained by utilizing socket-image's function, which is called gray comatrix. For GLCM feature extraction, the researchers compute 13 Haralick features (contrast, energy, homogeneity, and others) across 4 angles (0°, 45°, 90°, 135°) and 3 pixel distances (1, 3, 5) using overlapping 32×32 patches (50% overlap), generating 1,476-dimensional feature vectors per image. DTDWT features are extracted via 3-level decomposition (Q-shift filters), yielding 72-dimensional mean/variance descriptors of subband coefficients.

The DTDWT implementation leverages Colab's Graphics Processing Unit (GPU) acceleration through the CuPy-optimized dtcwt package. Three levels of decomposition are conducted on each MRI scan, using near-symmetric Q-shift filters. It results in 6 directional subbands per level. To execute the experiment, Colab's high-Random Access Memory (RAM) mode (24 GB) is utilized to handle memory-intensive wavelet computations. Mean and variance of coefficient magnitudes are computed for each subband, generating a 72-dimensional feature vector per image.

For the t-SNE analysis, Colab's GPU-accelerated implementation from scikit-learn is used, reducing the combined 1,476-dimensional GLCM and DTDWT features to 13 dimensions. A feature cache system is constructed that stores them on Google Drive after every successful run and includes checksums to verify data integrity, so that t-SNE results can be replicated.

For dimensionality reduction, the combined 1,476-D feature vectors are processed with t-SNE (perplexity= 25, learning_rate= 200, and n_components= 32) exclusively on the training set to prevent data leakage. The reduced features are used to construct k-NN graphs (k= 8 edges/node) where nodes represent Simple Linear Iterative Clustering (SLIC) superpixels (256 per image), and edges encode spatial proximity (10mm threshold). The GCN architecture comprises three graph convolutional layers (64→32→16 channels) with batch normalization, Rectified Linear Unit (ReLU) activation, and dropout (p= 0.3). Training uses AdamW(lr= $3e^{-4}$, weight_decay= $1e^{-4}$), with label smoothing (α= 0.1), and 50 epochs.

TABLE II
EXPERIMENTAL SETUP FOR TRAINING PARAMETERS.

Parameters	Value
Learning rate	3×10^{-4} (AdamW)
Batch size	8 (GCN), 32 (CNN)
Epoch	40
Hidden dimensions	[64, 32, 16]
Dropout rate	0.3
t-SNE dimensions	32

Note: Convolutional Neural Network (CNN), Graph Convolutional Network (GCN), and t-Distributed Stochastic Neighbor Embedding (t-SNE).

The evaluation of the dataset is achieved by splitting it into a training and test set with an 80/20 split ratio. It enables reliable model training and validation. This division not only ensures that there is enough data for training, but also allocates a specific amount of unseen data to be evaluated. After the feature extraction step, a graph-based deep learning method, GCN is applied to distinguish the affected breast from the normal breast.

A total of 255 embedding spaces are used to embed the MRI images. The graph-based architecture has hidden layers for the GCN that are configured with 32 and 64 units, respectively. The two hidden layers are equipped with ReLU activation functions, while the output layer uses the softmax function for binary classification. The categorical cross-entropy loss function is employed to train the model, which is then optimized with the Adam optimization method. Table II provides a summary of the experimental setup for training parameters.

III. RESULTS AND DISCUSSION

The proposed method holds great potential for the detection of breast cancer and the accurate classification of breast MRI images. It utilizes a combination of GLCM and DTDWT for feature extraction. After feature extraction, t-SNE is used to reduce the dimensionality of the data and improve efficiency. Finally, GCN is employed for classification. For evaluation purposes, four kernel types are employed: Radial Basis Function (RBF), linear, polynomial, and quadratic.

The analysis is done on four distinct 256×256 image datasets: (i) DC MRI image, (ii) lipoma MRI

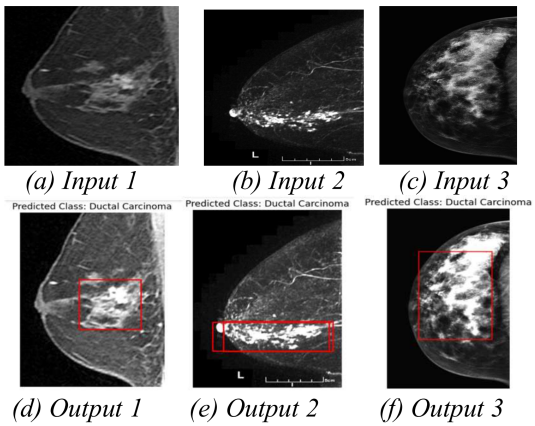

Fig. 3. (A-C) the input of breast Magnetic Resonance Imaging (MRI) image and (D-F) the output of the cancer region and Ductal Carcinoma (DC) classification.

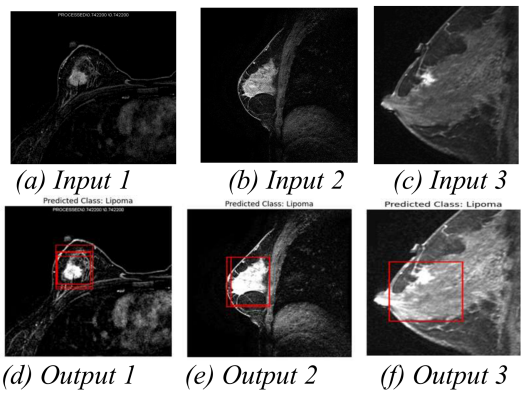

Fig. 4. (A-C) the input of breast Magnetic Resonance Imaging (MRI) image and (D-F) the output of the cancer region and lipoma classification.

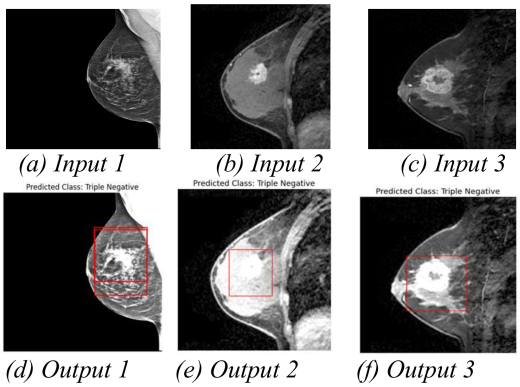

Fig. 5. (A-C) the input of breast Magnetic Resonance Imaging (MRI) image and (D-F) the output of cancer region and Triple-Negative Breast Cancer (TNBC) classification.

image, (iii) TNBC MRI image, and (iv) IBC MRI image. Accurate segmentation of breast MRI images is essential for the identification and diagnosis of

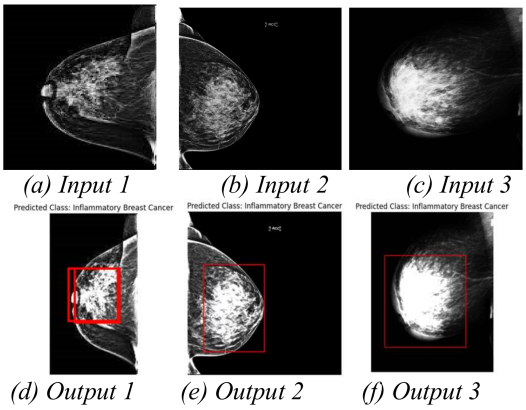

Fig. 6. (A-C) the input of breast Magnetic Resonance Imaging (MRI) image and (D-F) the output of cancer region and Inflammatory Breast Cancer (IBC) classification.

abnormalities. A random selection process is used. It randomly selects abnormal breast MRI images from a dataset and classifies them based on their likelihood of containing cancerous tissue.

Recognizing the distinction between benign and malignant cancers is crucial, as benign cancers are usually stationary and can be safely removed by surgery. Compared to benign cancers, malignant cancers are very aggressive and quickly spread to neighbouring tissues. The usual treatment for patients with malignant cancers is radiation therapy and chemotherapy to eliminate their cancer cells. Furthermore, malignant cancers frequently recur after treatment and are unlikely to be cured. In these situations, physicians concentrate on controlling symptoms and extending the patient's lifespan. The effectiveness of this treatment is significantly influenced by the accuracy of detection. By utilizing this approach, it is possible to distinguish benign cancers from malignant cancers on MRI images, which is a reliable tool for enhancing diagnostic accuracy and patient outcomes. This method leverages a hybrid framework that integrates GLCM for extracting texture-based features like contrast, energy, and homogeneity, alongside DTDWT for frequency-based edge preservation, ensuring a comprehensive representation of tissue characteristics. These features are then reduced in dimensionality using t-SNE to improve interpretability and efficiency, before being processed by a GCN that models relational dependencies for precise classification. This integrated framework enables precise differentiation between benign and malignant cases, while also facilitating categorization into key subtypes including DC, lipoma, TNBC, and IBC, ultimately aiding in earlier detection and more informed clinical decision-making.

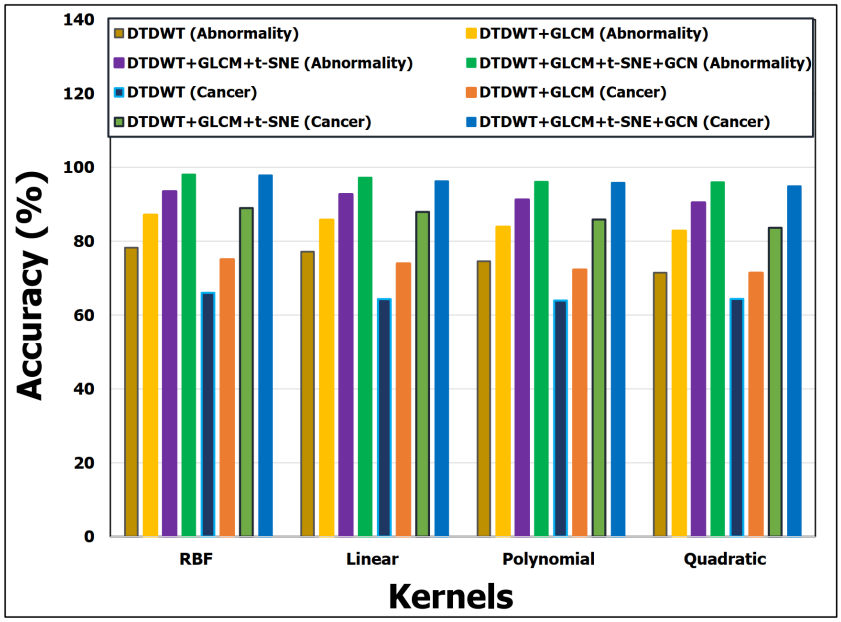

Fig. 7. Average accuracy in abnormality and cancer detection using Ductal Carcinoma (DC) Magnetic Resonance Imaging (MRI) image. Note: Gray-Level Co-Occurrence Matrix (GLCM), Graph Convolutional Network (GCN), t-Distributed Stochastic Neighbor Embedding (t-SNE), and Dual-Tree Discrete Wavelet Transform (DTDWT).

TABLE III
AVERAGE ACCURACY FOR DUCTAL CARCINOMA (DC) MAGNETIC RESONANCE IMAGING (MRI) IMAGES.

Classification	Method	DC MRI Images			
		RBF (%)	Linear (%)	Polynomial (%)	Quadratic (%)
Abnormality Classification	GLCM	78.23	77.16	74.56	71.46
	GLCM+DTDWT	87.12	85.76	83.87	82.76
	GLCM+DTDWT+t-SNE	93.45	92.67	91.21	90.45
	GLCM+DTDWT+t-SNE+GCN	98.07	97.22	96.08	95.97
Cancer Classification	GLCM	66.00	64.33	63.92	64.34
	GLCM+DTDWT	75.02	73.91	72.23	71.38
	GLCM+DTDWT+t-SNE	88.95	87.91	85.89	83.62
	GLCM+DTDWT+t-SNE+GCN	97.82	96.25	95.82	94.89

Note: Gray-Level Co-Occurrence Matrix (GLCM), Graph Convolutional Network (GCN), t-Distributed Stochastic Neighbor Embedding (t-SNE), and Dual-Tree Discrete Wavelet Transform (DTDWT).

A. Simulation and Observation/Output of Simulation

The results (as depicted in Figs. 3–6) are obtained by simulating each image. This demonstration is focused on accurately classifying breast cancer cases and analyzing the performance patterns of the proposed algorithm. The goal is to achieve correct classifications and evaluate how the method distinguishes between different categories. In particular, the visualizations illustrate the separability of feature representations and the consistency of prediction outcomes across the test samples. These also provide insight into the model's ability to capture discriminative texture and structural characteristics from MRI images for reliable decision-making. These visual outcomes present evidence of the GCN's ability to capture subtle texture and structural differences in MRI images, which supports the claim of superior diagnostic performance compared to traditional approaches. Overall, this simulation-based evaluation underscores the robustness of the integrated GLCM-DTDWT-t-SNE-GCN pipeline in handling real-world variations in breast MRI data.

B. Evaluation of the Model using Ductal Carcinoma (DC) MRI Image Dataset

Figure 7 and Table III show the classification of abnormalities within DC MRI image. The dataset for classifying DC is constructed from 200 images, where 160 images are used for training, and 40 images are utilized for validation. By performing simulations on selected images, the proposed method allows the researchers to distinguish between normal breast tissues

TABLE IV
AVERAGE ACCURACY FOR LIPOMA MAGNETIC RESONANCE IMAGING (MRI) IMAGES.

Classification	Method	Lipoma MRI Images			
		RBF (%)	Linear (%)	Polynomial (%)	Quadratic (%)
Abnormality Classification	GLCM	78.23	77.76	75.86	73.11
	GLCM+DTDWT	85.12	83.06	82.37	81.26
	GLCM+DTDWT+t-SNE	90.45	89.37	88.31	87.05
	GLCM+DTDWT+t-SNE+GCN	98.07	97.92	96.88	95.58
Cancer Classification	GLCM	70.81	68.33	67.02	64.44
	GLCM+DTDWT	78.32	76.81	75.33	73.88
	GLCM+DTDWT+t-SNE	91.05	89.31	87.89	86.98
	GLCM+DTDWT+t-SNE+GCN	97.82	96.25	95.12	94.09

Note: Gray-Level Co-Occurrence Matrix (GLCM), Graph Convolutional Network (GCN), t-Distributed Stochastic Neighbor Embedding (t-SNE), and Dual-Tree Discrete Wavelet Transform (DTDWT).

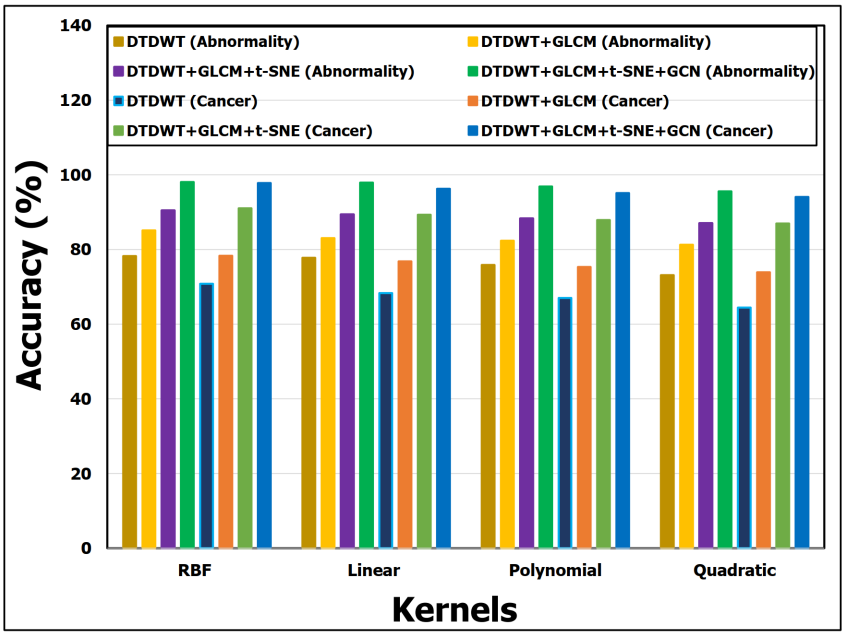

Fig. 8. Average accuracy in abnormality and cancer detection using lipoma Magnetic Resonance Imaging (MRI) image. Note: Gray-Level Co-Occurrence Matrix (GLCM), Graph Convolutional Network (GCN), t-Distributed Stochastic Neighbor Embedding (t-SNE), and Dual-Tree Discrete Wavelet Transform (DTDWT).

and abnormal ones. A comprehensive assessment of the classification outcomes, including accuracy measurement, has been provided for four kernels: RBF, linear, polynomial, and quadratic, as shown in Table III and Fig. 7. The method is proven to be successful in distinguishing normal from abnormal breast MRI images.

For cancer classification of DC MRI Images, normal and cancerous breasts are first identified and classified. In the second step, four types of cancer are classified by analyzing the patterns of only cancerous images. In determining the cancer pattern, each class of cancer has been taken into account. In the case of DC, 60 malignant breasts are taken for the training set. Then, 16 malignant breasts are taken for the validation set. The designed simulation is able to accurately classify DC breast cancer. The mathematical analysis is detailed in Fig. 7.

C. Evaluation of the Model using Lipoma Magnetic Resonance Imaging (MRI) Image Dataset

The dataset used to classify lipoma MRI images consists of 200 images, of which 160 are used for training and 40 for validation. The proposed method distinguishes between normal and abnormal breast tissue with the use of simulated images of selected cases. Table IV and Fig. 8 demonstrate the detailed results of a comprehensive evaluation of classification performance for four kernel methods: RBF, linear kernel, polynomial kernel, and quadratic kernel. The results

Cite this article as: F. A. Jibon, S. C. Roy, H. R. Mou, M. A. Islam, U. K. Das, R. Sarkar, and R. R. Sarkar, "Magnetic Resonance Imaging (MRI)-based breast cancer detection using Graph Convolutional Network (GCN) with advanced texture feature extraction", CommIT Journal 20(1), 29–44, 2026.

TABLE V
AVERAGE ACCURACY FOR TRIPLE-NEGATIVE BREAST CANCER (TNBC) MAGNETIC RESONANCE IMAGING (MRI) IMAGES

Classification	Method	TNBC MRI Images			
		RBF (%)	Linear (%)	Polynomial (%)	Quadratic (%)
Abnormality Classification	GLCM	77.88	76.67	75.42	73.71
	GLCM+DTDWT	86.42	84.06	83.57	81.26
	GLCM+DTDWT+t-SNE	91.35	88.97	87.25	86.62
	GLCM+DTDWT+t-SNE+GCN	99.05	98.25	97.78	96.76
Cancer Classification	GLCM	72.61	70.65	68.32	66.75
	GLCM+DTDWT	86.32	85.81	84.37	81.73
	GLCM+DTDWT+t-SNE	96.05	95.41	94.59	92.65
	GLCM+DTDWT+t-SNE+GCN	98.80	97.66	96.86	95.77

Note: Gray-Level Co-Occurrence Matrix (GLCM), Graph Convolutional Network (GCN), t-Distributed Stochastic Neighbor Embedding (t-SNE), and Dual-Tree Discrete Wavelet Transform (DTDWT).

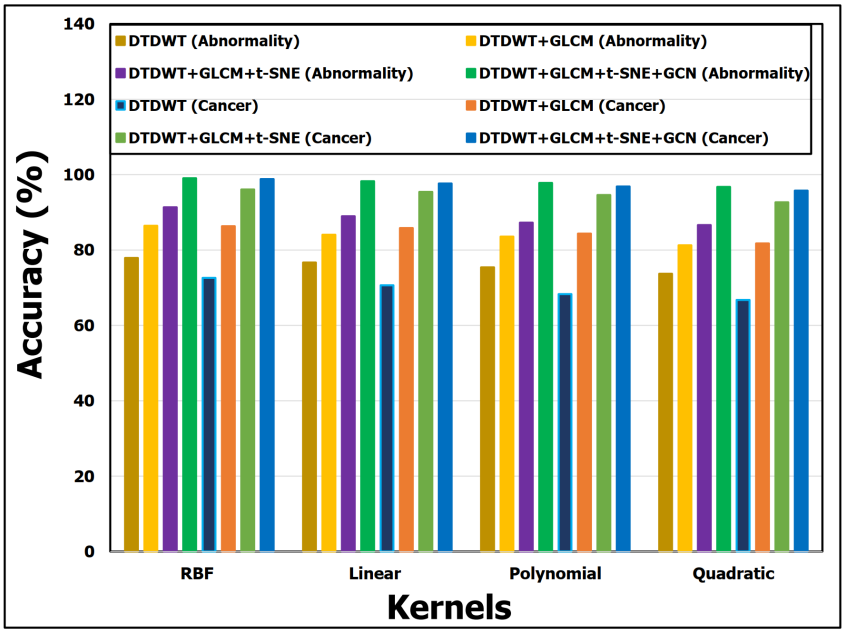

Fig. 9. Average accuracy in abnormality and cancer detection using Triple-Negative Breast Cancer (TNBC) Magnetic Resonance Imaging (MRI) image. Note: Gray-Level Co-Occurrence Matrix (GLCM), Graph Convolutional Network (GCN), t-Distributed Stochastic Neighbor Embedding (t-SNE), and Dual-Tree Discrete Wavelet Transform (DTDWT).

confirm that the accuracy improvement for detection and cancer classification for all kernels is achieved by using GLCM, DTDWT, SNE, and GCN methods, leading to continuous improvements.

For lipoma MRI image cancer classification, the experimental procedure uses a two-phase classification procedure similar to DC analysis. The initial task is to distinguish normal breast tissue from abnormal lipoma cases by using binary classification. Subsequently, a detailed classification of four specific malignancy types is conducted by analyzing patterns in confirmed cancerous lipoma images. In order to maintain consistency with the other cancer analyses, the training set contains 60 malignant lipoma cases, and the validation set includes 16 cases. The results shown in Fig. 8 confirm the method's robustness across different breast pathology types. The combined GLCM+DTDWT+t-SNE+GCN approach consistently delivers superior performance for lipoma cancer classification tasks.

D. Evaluation of the Model Using Triple-Negative Breast Cancer (TNBC) Magnetic Resonance Imaging (MRI) Image Dataset

The dataset for the classification of TNBC MRI images includes 160 images for training and 40 for validation. A comprehensive evaluation of classification performance performed for four kernel methods similar to DC and Lipoma is shown in Table V and Fig. 9, with detailed results. It is confirmed from the results that integrating GLCM, DTDWT, SNE,

TABLE VI
AVERAGE ACCURACY FOR INFLAMMATORY BREAST CANCER (IBC) MAGNETIC RESONANCE IMAGING (MRI) IMAGES

Classification	Method	IBC MRI Images			
		RBF (%)	Linear (%)	Polynomial (%)	Quadratic (%)
Abnormality Classification	GLCM	79.23	78.76	77.86	75.11
	GLCM+DTDWT	85.12	83.06	82.37	81.26
	GLCM+DTDWT+t-SNE	90.45	89.37	88.31	87.05
	GLCM+DTDWT+t-SNE+GCN	98.07	97.92	96.88	95.58
Cancer Classification	GLCM	70.81	68.33	67.02	64.44
	GLCM+DTDWT	78.32	76.81	75.33	73.88
	GLCM+DTDWT+t-SNE	91.05	89.31	87.89	86.98
	GLCM+DTDWT+t-SNE+GCN	97.82	96.25	95.12	94.09

Note: Gray-Level Co-Occurrence Matrix (GLCM), Graph Convolutional Network (GCN), t-Distributed Stochastic Neighbor Embedding (t-SNE), and Dual-Tree Discrete Wavelet Transform (DTDWT).

and GCN methods results in continuous improvements for TNBC abnormality and cancer classification for all kernels. TNBC's superior performance is due to GLCM's capacity to comprehend TNBC's distinctive texture patterns, DTDWT's efficacy in evaluating its irregular tumor margins across multiple levels, t-SNE's capability to manage TNBC's high-dimensional feature space, and GCN's ability to model its complex spatial relationships.

For TNBC MRI image cancer classification, the experimental approach is a two-stage classification framework similar to the DC and Lipoma analyses. A total of 60 TNBC cases are allocated for training and 16 cases for validation to ensure methodological consistency with the other studies. Figure 9 demonstrates the effectiveness of the method for this aggressive breast cancer classification. The integrated GLCM+DTDWT+SNE+GCN method is particularly effective in TNBC classification because it is capable of capturing TNBC's characteristic irregular tumor morphology through DTDWT's multi-scale analysis, handling its heterogeneous imaging patterns through t-SNE's dimensionality reduction, and modelling its aggressive spatial growth patterns using GCNs.

E. Evaluation of the Model Using Inflammatory Breast Cancer (IBC) Magnetic Resonance Imaging (MRI) Image Dataset

The IBC MRI image dataset is designed to identify breast image abnormalities. It comprises 160 images for training and 40 for validation. The technique is evaluated in experiments to assess its ability to distinguish between normal and abnormal cases. Table VI and Fig. 10 demonstrate the approach's ability to detect abnormalities in breast MRI images accurately. The results can confirm that the combination of GLCM, DTDWT, t-SNE, and GCN performs better than all other combinations for all types of kernels.

For IBC MRI image cancer classification, identical approaches to those used in the DC, Lipoma, and TNBC studies are employed. The use of 60 images for training and 16 images for validation of malignant cases helps the researchers to maintain methodological consistency across cancer classification. The simulation framework is able to achieve a precise classification of the IBC, with complete performance metrics and methodological details, shown in Fig. 10. These results confirm that this approach can tackle IBC diagnostic issues through multi-scale feature analysis and spatial relationship modelling.

F. Discussion

Table VII presents a performance comparison between this proposal and existing methods, focusing exclusively on accuracy metrics for breast cancer detection and classification tasks. This results highlights how the proposed hybrid framework integrating GCN with advanced feature extraction techniques: GLCM, DTDWT, and t-SNE stacks up against prior state-of-the-art approaches across various datasets and models. Compared to prior works, it outperforms models like DUALCORENET (93% on INbreast, 85% on Digital Database for Screening Mammography (DDSM)) [17], You Only Look Once-based Computer-Aided Detection/Diagnosis system (YOLO-based CAD) (95% on INbreast) [18], basic GCN (81% on Mammographic Image Analysis Society database (MIAS)) [22], ResHist (84.34% on BreakHis) [31], Deep Learning Assisted Efficient AdaBoost Algorithm (DLA-EABA) (97.2% on private) [32], and ResNet-50 (93% on INbreast) [33], while being competitive with U-Net 3+ (98.47% on INbreast) [16]. This superiority arises from the method's ability to integrate complementary multi-scale features and graph-based propagation.

The main contributions of this proposal are summarized as follows. First, a graph-based hybrid deep

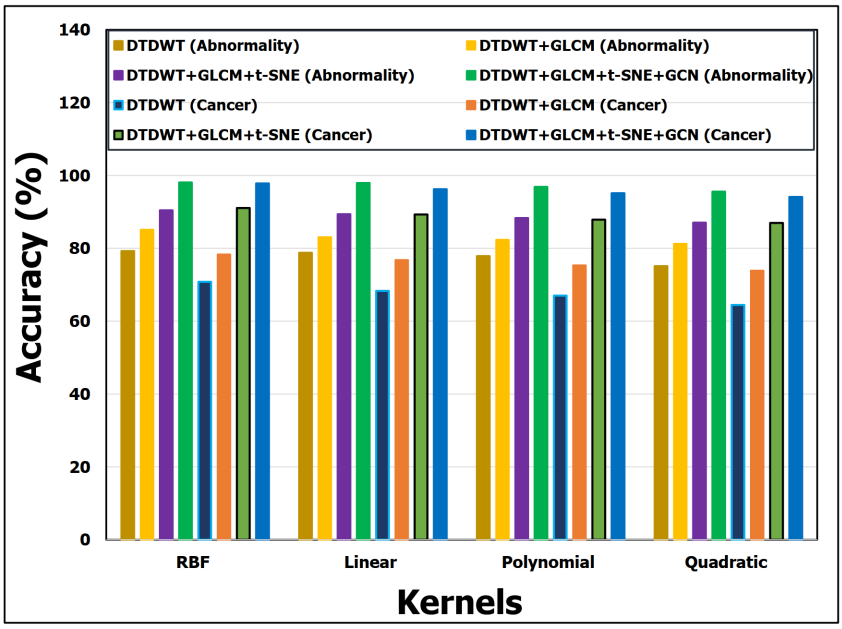

Fig. 10. Average accuracy in abnormality and cancer detection using Inflammatory Breast Cancer (IBC) Magnetic Resonance Imaging (MRI) image. Note: Gray-Level Co-Occurrence Matrix (GLCM), Graph Convolutional Network (GCN), t-Distributed Stochastic Neighbor Embedding (t-SNE), and Dual-Tree Discrete Wavelet Transform (DTDWT).

TABLE VII
ASSESSMENT OF PERFORMANCE AGAINST EXISTING METHODS BASED ON ACCURACY.

Ref.	Dataset	Learning Approach/Model	Feature Extraction Techniques	Prediction Classes	Accuracy
[16]	INbreast FFDM	U-Net 3+	-	Benign/Malignant	0.9847
[17]	INbreast	DUALCORENET	LPL and CGL	Benign/Malignant	0.9300
[18]	INbreast	YOLO-based CAD system	-	Benign/Malignant	0.9500
[22]	MIAS	GCN	ROIs Crop	Benign/Malignant	0.8100
[31]	BreaKHis	ResHist	-	Benign/Malignant	0.8434
[32]	Private	DLA-EABA	-	Benign/Malignant/Normal	0.9720
[33]	INbreast	ResNet-50 CNN	-	Benign/Malignant	0.9300
Proposal	Private	GCN	DTDWT+GLCM+t-SNE	Benign/Malignant	0.9821

Note: Convolutional Neural Network (CNN), Gray-Level Co-Occurrence Matrix (GLCM), Graph Convolutional Network (GCN), t-Distributed Stochastic Neighbor Embedding (t-SNE), Dual-Tree Discrete Wavelet Transform (DTDWT), Full-Field Digital Mammography (FFDM), Mammographic Image Analysis Society database (MIAS), You Only Look Once-based Computer-Aided Detection/Diagnosis system (YOLO-based CAD), Deep Learning Assisted Efficient AdaBoost Algorithm (DLA-EABA), Locality Preserving Learner (LPL), Conditional Graph Learner (CGL), and Region of Interest (ROI).

learning method is proposed that can efficiently detect and classify four types of breast cancer. Second, by combining GLCM's powerful texture analysis with DTDWT's superior edge and detail preservation, this hybrid approach improves classification accuracy, enabling more precise identification of cancerous regions. Third the combination of t-SNE with GLCM and DTDWT enhances breast cancer detection by improving feature representation and visualization. Last, by evaluating benchmark datasets, a comprehensive evaluation shows that the proposed framework has superior performance when compared to state-of-the-art methods.

IV. CONCLUSION

In the research, GCN is proposed as a ML-framework designed for breast MRI image classification. The classification system effectively distinguishes cancerous from non-cancerous cases by accurately separating benign cancer from malignant ones. The implementation involves the incorporation of texture features into GLCM and DTDWT, t-SNE-based dimensionality reduction, and graph convolutional networks for classification. The developed classification approach demonstrates effectiveness in MRI image classification for DC, lipoma, TNBC, and IBC while handling both neoplastic and degenerative cancer types. The experimental results confirm that the integrated GLCM+DTDWT+t-SNE+GCN framework

consistently outperforms conventional feature extraction and classification methods. The proposed model achieves an average classification accuracy of 98.21%, with cancer detection accuracies of 97.82% for DC, 97.82% for lipoma, 98.80% for TNBC, and 97.82% for IBC across multiple kernel functions (RBF, linear, polynomial, and quadratic). These outcomes demonstrate the robustness, reliability, and generalizability of the proposed method, underscoring its potential as a dependable diagnostic tool in medical imaging.

Although the proposed breast cancer diagnosis method demonstrates promising performance in distinguishing benign from malignant tissues and classifying key subtypes on MRI images, it requires validation on larger, more diverse, multi-center datasets to confirm generalizability, address potential biases, and meet clinical and regulatory standards for approval. Future efforts can prioritize such large-scale prospective testing, external validation across diverse imaging protocols and populations, and real-world performance assessment to support safe and effective clinical integration. In addition, future research can examine the transferability of this hybrid approach leveraging GLCM texture features, DTDWT multi-resolution analysis, t-SNE dimensionality reduction, and GCN relational modeling to additional malignancies, including lung, colon, and prostate cancer, to determine its broader utility in multi-cancer early detection and precision oncology.

Author Contribution

Conceived and designed the analysis, S. C. R. and M. A. I.; Collected the data, F. A. J., S. C. R., and R. R. S.; Contributed data or analysis tools, F. A. J., S. C. R., and R. S.; Performed the analysis, F. A. J., S. C. R., and H. R. M.; and Wrote the paper, S. C. R., M. A. I., and U. K. D.

Data Availability

The data that support the findings of the research are openly available in https://radiopaedia.org/articles/breast-mri

References

[1] T. M. Allweis, N. Hermann, R. Berenstein-Molho, and M. Guindy, "Personalized screening for breast cancer: Rationale, present practices, and future directions," *Annals of Surgical Oncology*, vol. 28, no. 8, pp. 4306–4317, 2021.

[2] M. Arnold, E. Morgan, H. Rumgay, A. Mafra, D. Singh, M. Laversanne, J. Vignat, J. R. Gralow, F. Cardoso, S. Siesling, and I. Soerjomataram, "Current and future burden of breast cancer: Global statistics for 2020 and 2040," *The Breast*, vol. 66, pp. 15–23, 2022.

[3] M. M. Srikantamurthy, V. P. S. Rallabandi, D. B. Dudekula, S. Natarajan, and J. Park, "Classification of benign and malignant subtypes of breast cancer histopathology imaging using hybrid CNN-LSTM based transfer learning," *BMC Medical Imaging*, vol. 23, pp. 1–15, 2023.

[4] C. Xu, Z. Gu, J. Liu, X. Lin, C. Wang, J. Li, Y. Fu, X. Cheng, and Z. Zhuang, "Adenosquamous carcinoma of the breast: A population-based study," *Breast Cancer*, vol. 28, no. 4, pp. 848–858, 2021.

[5] H. M. T. Khushi, T. Masood, A. Jaffar, and S. Akram, "A novel approach to classify brain tumor with an effective transfer learning based deep learning model," *Brazilian Archives of Biology and Technology*, vol. 67, pp. 1–18, 2024.

[6] S. S. Reddy, N. Pilli, P. Voosala, and S. R. Chigurupati, "A comparative study to predict breast cancer using machine learning techniques," *Indonesian Journal of Electrical Engineering and Computer Science (IJEECS)*, vol. 27, no. 1, pp. 171–180, 2022.

[7] F. A. Jibon, M. U. Khandaker, M. H. Miraz, H. Thakur, F. Rabby, N. Tamam, A. Sulieman, Y. S. Itas, and H. Osman, "Cancerous and non-cancerous brain MRI classification method based on convolutional neural network and log-polar transformation," *Healthcare*, vol. 10, no. 9, pp. 1–19, 2022.

[8] G. Holste, S. C. Partridge, H. Rahbar, D. Biswas, C. I. Lee, and A. M. Alessio, "End-to-end learning of fused image and non-image features for improved breast cancer classification from MRI," in *Proceedings of the IEEE/CVF International Conference on Computer Vision*, Virtual, Oct. 11–17, 2021, pp. 3294–3303.

[9] H. Chen, N. Wang, X. Du, K. Mei, Y. Zhou, and G. Cai, "Classification prediction of breast cancer based on machine learning," *Computational Intelligence and Neuroscience*, vol. 2023, no. 1, pp. 1–9, 2023.

[10] S. Nanglia, M. Ahmad, F. A. Khan, and N. Z. Jhanjhi, "An enhanced predictive heterogeneous ensemble model for breast cancer prediction," *Biomedical Signal Processing and Control*, vol. 72, 2022.

[11] M. J. Khan, A. K. Singh, R. Sultana, P. P. Singh, A. Khan, and S. Saxena, "Breast cancer: A comparative review for breast cancer detection using machine learning techniques," *Cell Biochemistry and Function*, vol. 41, no. 8, pp. 996–1007, 2023.

[12] J. O. Afolayan, M. O. Adebiyi, M. O. Arowolo, C. Chakraborty, and A. A. Adebiyi, "Breast cancer detection using particle swarm optimization and decision tree machine learning technique," in *Intelligent healthcare: Infrastructure, algorithms and management*. Springer, 2022, pp. 61–83.

[13] M. Darwich and M. Bayoumi, "An evaluation of the effectiveness of machine learning prediction models in assessing breast cancer risk," *Informatics in Medicine Unlocked*, vol. 49, pp. 1–17, 2024.

[14] J. Wang, M. A. Khan, S. Wang, and Y. Zhang, "SNSVM: SqueezeNet-guided SVM for breast cancer diagnosis," *Computers, Materials & Continua*, vol. 76, no. 2, pp. 2201–2216, 2023.

[15] R. Jalloul, C. H. Krishnappa, V. I. Agughasi, and R. Alkhatib, "Enhancing early breast cancer detection with infrared thermography: A comparative evaluation of deep learning and machine learning models," *Technologies*, vol. 13, no. 1, pp. 1–31, 2024.

[16] B. S. Abunasser, M. R. J. Al-Hiealy, I. S. Zaqout, and S. S. Abu-Naser, "Convolution neural network for breast cancer detection and classification using deep learning," *Asian Pacific Journal of Cancer Prevention: APJCP*, vol. 24, no. 2, pp. 531–544, 2023.

[17] S. M. Shaaban, M. Nawaz, Y. Said, and M. Barr, "An efficient breast cancer segmentation system based on deep learning techniques," *Engineering, Technology & Applied Science Research*, vol. 13, no. 6, pp. 12 415–12 422, 2023.

[18] H. Li, D. Chen, W. H. Nailon, M. E. Davies, and D. I. Laurenson, "Dual convolutional neural networks for breast mass segmentation and diagnosis in mammography," *IEEE Transactions on Medical Imaging*, vol. 41, no. 1, pp. 3–13, 2021.

[19] R. M. Munshi, L. Cascone, N. Alturki, O. Saidani, A. Alshardan, and M. Umer, "A novel approach for breast cancer detection using optimized ensemble learning framework and XAI," *Image and Vision Computing*, vol. 142, 2024.

[20] H. Aljuaid, N. Alturki, N. Alsubaie, L. Cavallaro, and A. Liotta, "Computer-aided diagnosis for breast cancer classification using deep neural networks and transfer learning," *Computer Methods and Programs in Biomedicine*, vol. 223, pp. 1–10, 2022.

[21] S. S. Chowa, S. Azam, S. Montaha, I. J. Payel, M. R. I. Bhuiyan, M. Z. Hasan, and M. Jonkman, "Graph neural network-based breast cancer diagnosis using ultrasound images with optimized graph construction integrating the medically significant features," *Journal of Cancer Research and Clinical Oncology*, vol. 149, no. 20, pp. 18 039–18 064, 2023.

[22] S. A. Shanto, G. K. Paul, R. A. Mohon, S. Sarker, M. S. Mahir, and S. S. Haque, "Machine learning in healthcare: Breast cancer detection using graph convolutional network," *International Journal of Research and Innovation in Applied Science (IJRIAS)*, vol. 7, no. 8, pp. 78–86, 2022.

[23] Y. Cakmak, S. Safak, M. A. Bayram, and I. Pacal, "Comprehensive evaluation of machine learning and ANN models for breast cancer detection," *Computer and Decision Making: An International Journal*, vol. 1, pp. 84–102, 2024.

[24] J. Chen, J. Ou, H. Zeng, and C. Cai, "A fast algorithm based on gray level co-occurrence matrix and Gabor feature for HEVC screen content coding," *Journal of Visual Communication and Image Representation*, vol. 78, p. 103128, 2021.

[25] C. Chiappa, A. Bonetti, G. J. Jaber, V. De Berardinis, V. Bianchi, and F. Rovera, "Pure ductal carcinoma in situ of the breast: Analysis of 270 consecutive patients treated in a 9-year period," *Cancers*, vol. 13, no. 3, pp. 1–16, 2021.

[26] G. M. Wilson, P. Dinh, N. Pathmanathan, and J. D. Graham, "Ductal carcinoma in situ: Molecular changes accompanying disease progression," *Journal of Mammary Gland Biology and Neoplasia*, vol. 27, no. 1, pp. 101–131, 2022.

[27] L. Kolb, S. N. S. Yarrarapu, and J. A. Rosario-Collazo, "Lipoma," 2023. [Online]. Available: https://www.ncbi.nlm.nih.gov/books/NBK507906

[28] R. A. Towner, R. Dissanayake, and M. Ahmed, "Clinical advances in triple negative breast cancer treatment: Focus on poly (l-lactide-coglycolide) nanoparticles," *The Journal of Pharmacology and Experimental Therapeutics*, vol. 390, no. 1, pp. 53–64, 2024.

[29] D. Sood, C. Kaur, N. Kumar, R. Kumar, and G. Singh, "Triple-negative breast cancer: Challenges, advances, and promising therapeutic interventions," *Medical Oncology*, vol. 42, p. 506, 2025.

[30] R. Salmanzadeh, K. Aghemo, B. Thatiparthi, S. A. Al-Shaikhli, A. Salmanzadeh, O. DeAngelo, D. Martin, S. Sukpraprut-Braaten, A. M. Salmanzadeh, and D. E. Martin, "A case of advanced bilateral inflammatory breast cancer: A radiological perspective," *Cureus*, vol. 15, no. 1, pp. 1–7, 2023.

[31] M. Gour, S. Jain, and T. Sunil Kumar, "Residual learning based CNN for breast cancer histopatho-

logical image classification," *International Journal of Imaging Systems and Technology*, vol. 30, no. 3, pp. 621–635, 2020.

[32] J. Zheng, D. Lin, Z. Gao, S. Wang, M. He, and J. Fan, "Deep learning assisted efficient AdaBoost algorithm for breast cancer detection and early diagnosis," *IEEE Access*, vol. 8, pp. 96 946–96 954, 2020.

[33] H. Rahman, T. F. Naik Bukht, R. Ahmad, A. Almadhor, and A. R. Javed, "Efficient breast cancer diagnosis from complex mammographic images using deep convolutional neural network," *Computational Intelligence and Neuroscience*, vol. 2023, no. 1, pp. 1–11, 2023.